The Effect of a Coastal Shelf on Long Waves in a Rotating Hemispherical Basin[1]

Niels Christensen, Jr.

Hawaii Institute of Geophysics
University of Hawaii
Honolulu, Hawaii 96822

ABSTRACT

Using finite difference methods, the effect on long waves of a coastal shelf in a rotating hemispherical basin, symmetric about the equator, is studied. Of the four modes investigated, with a shelf added to a constant-depth basin, two modes respond weakly: one is a planetary mode antisymmetric in the sea surface about the equator; the other is a gravity mode symmetric in the sea surface. The other two modes were affected strongly but differently: one, a symmetric planetary mode, increases in frequency, and the wave moves onto the shelf; the other, a symmetric gravity mode, decreases in frequency and its wave moves away from the shelf.

Introduction. In this paper, free barotropic oscillations in a hemispherical ocean centered on the equator of a rotating earth are investigated as a coastal shelf is added. The earth's sphericity and horizontal divergence are properly accounted for. The purpose is to study the effect on long waves of a feature such as the continental shelf.

Veronis (1966), Longuet-Higgins (1968), Buchwald (1969), Rhines (1969), and others have considered the effect of bottom topography on long waves. Variously, they have shown that even minor topography can strongly affect these waves. In this paper, it is shown that different modes respond differently to a feature such as a shelf.

Finite difference techniques are employed to find the normal modes, each represented by a frequency and a surface wave. That is, after solving Laplace's equations for a single dependent variable, derivatives are replaced with finite differences. Boundary conditions are also expressed in finite differences, and the result is a set of linear homogeneous algebraic equations. Solutions of this set of equations are approximate normal modes of the basin being modeled.

1. Hawaii Institute of Geophysics Contribution No. 534.
Accepted for publication and submitted to press 3 May 1973.

First, four solutions are found for a hemispherical basin with a flat bottom. These solutions are tentatively identified by comparing them with solutions for similar basins found by Longuet-Higgins and Pond (1970), Mofjeld and Rattray (1971), and Christensen (1972). Two are planetary modes and two are gravity modes. Then, a shelf is allowed to rise slowly along the boundaries as the frequency and surface wave of a solution are monitored.

The Basic Equation. Laplace's equations are an adequate mathematical expression for long barotropic ocean waves. [See Lamb 1945 for a detailed derivation of these equations; also Hough (1898) or Eckart (1960) for a discussion of their validity.]

$$\left.\begin{aligned} \frac{\partial u}{\partial t} - 2\omega v \cos\theta &= -\frac{g}{a}\frac{\partial \zeta}{\partial \theta}. \\ \frac{\partial v}{\partial t} + 2\omega u \cos\theta &= -\frac{g}{a}\csc\theta\frac{\partial \zeta}{\partial \varphi}. \\ \frac{\partial \zeta}{\partial t} &= -\frac{1}{a}\csc\theta\left[\frac{\partial}{\partial \theta}(hu\sin\theta) + \frac{\partial}{\partial \varphi}(hv)\right]. \end{aligned}\right\} \quad (1)$$

Here a is the earth's radius, g is the acceleration of gravity, ω is the earth's angular velocity, θ and φ are colatitude and east longitude, respectively, u and v are horizontal orbital velocity components in the θ and φ directions, respectively, ζ is the elevation of the sea surface above its mean position, and h is the mean water depth.

The independent space variables θ and φ are already nondimensional. The following substitutions nondimensionalize the other variables and simplify equations (1):

$$\left.\begin{aligned} v &= a^{3/2} g^{1/2} h^{-1} U \csc\theta; \\ u &= -a^{3/2} g^{1/2} h^{-1} V \csc\theta; \\ \zeta &= \frac{1}{2} a^{1/2} g^{1/2} \omega^{-1} Z; \\ t &= \frac{1}{2}\omega^{-1}\tau; \\ h &= 4a^2\omega^2 g^{-1} H; \\ \sigma &= 2\omega\lambda. \end{aligned}\right\} \quad (2)$$

The frequency, σ, is introduced by assuming periodic motion and by setting all dependent variables proportional to $e^{-i\lambda\tau}$. The following equations result:

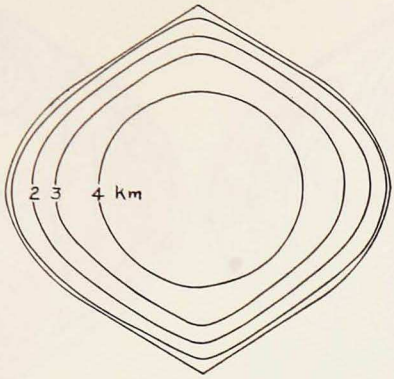

Figure 1. Depth contours for a shelved hemispherical basin.

$$\left.\begin{aligned} i\lambda U + \cos\theta V - H\frac{\partial Z}{\partial \varphi} &= 0; \\ \cos\theta U - i\lambda V - H\sin\theta\frac{\partial Z}{\partial \theta} &= 0; \\ \csc^2\theta\frac{\partial U}{\partial \varphi} - \csc\theta\frac{\partial V}{\partial \theta} - i\lambda Z &= 0. \end{aligned}\right\} \tag{3}$$

Eqs. (3) can be reduced to a single equation, with Z as the only dependent variable. Using the first two equations, U and V can be solved in terms of Z.

$$U = \Delta^{-1}H\left(i\lambda\frac{\partial Z}{\partial \varphi} + \cos\theta\sin\theta\frac{\partial Z}{\partial \theta}\right); \tag{4}$$

$$V = \Delta^{-1}H\left(-i\lambda\sin\theta\frac{\partial Z}{\partial \theta} + \cos\theta\frac{\partial Z}{\partial \varphi}\right); \tag{5}$$

here $\Delta = \cos^2\theta - \lambda^2$. Substituting these expressions for U and V into the third equation of (3) gives

$$\left.\begin{aligned} &\lambda\sin^2\theta\Delta^2 Z - \lambda\Delta\left[H\left(\frac{\partial^2 Z}{\partial \varphi^2} + \cos\theta\sin\theta\frac{\partial Z}{\partial \theta} + \sin^2\theta\frac{\partial^2 Z}{\partial \theta^2}\right) + \right. \\ &\left. + \frac{\partial H}{\partial \varphi}\frac{\partial Z}{\partial \varphi} + \sin^2\theta\frac{\partial H}{\partial \theta}\frac{\partial Z}{\partial \theta}\right] - i\Delta\cos\theta\sin\theta\left(-\frac{\partial H}{\partial \varphi}\frac{\partial Z}{\partial \theta} + \frac{\partial H}{\partial \theta}\frac{\partial Z}{\partial \varphi}\right) - \\ &- 2H\lambda\cos\theta\sin^3\theta\frac{\partial Z}{\partial \theta} - i\sin^2\theta(\cos^2\theta + \lambda^2)H\frac{\partial Z}{\partial \varphi} = 0. \end{aligned}\right\} \tag{6}$$

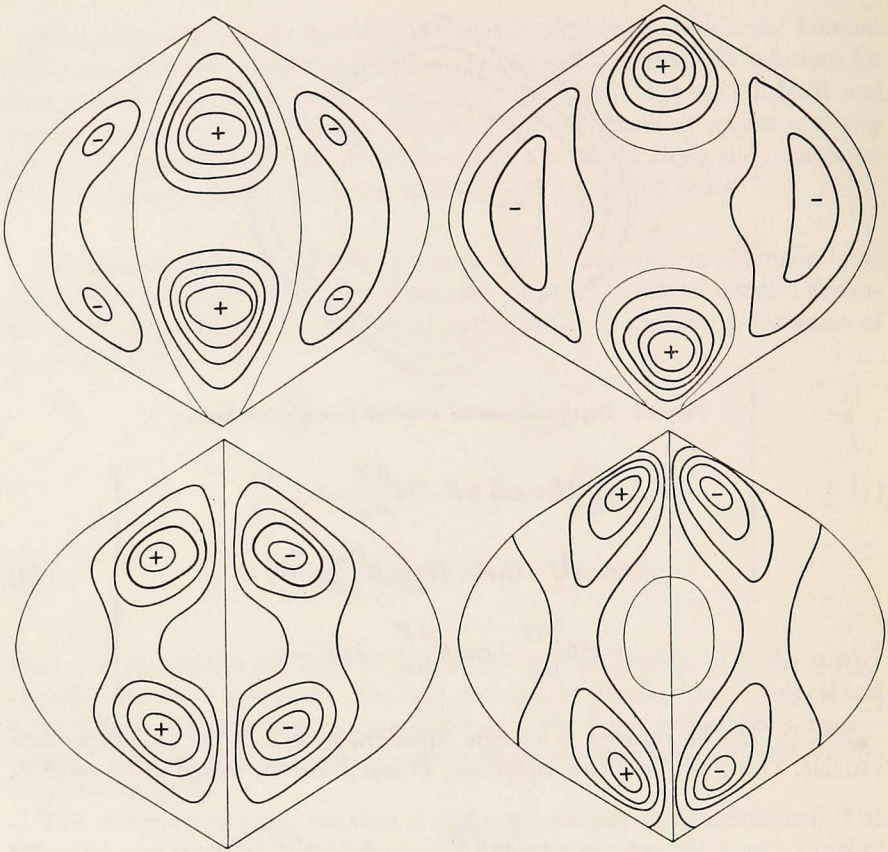

Figure 2a (left). Planetary oscillation $(1,2,p)$ with period = 168.6 hr for a hemisphere with h = 4 km everywhere. Figure 2b (right). Planetary oscillation $(1,2,p)$ with period = 107.4 hr for a hemisphere with a coastal shelf. Above: $\mathrm{Re}(Z)$. Below: $\mathrm{Im}(Z)$.

The Numerical Setup. Following is the general procedure used in finding the normal modes of a basin; the details are given in Christensen (1972): A grid of points, rectangular with respect to the independent space variables, θ and φ, represents the basin. Thus, the basin is a spherical rectangle (rectangular with respect to the coordinates, θ and φ), and the angular distance between the points in either direction is constant. One or more conditions on a single dependent variable applies at each point. Some points are interior points while others are boundary or corner points; the conditions will be different in each case.

At the interior points, the dynamic condition (6) is applied; at the east and west noncorner boundary points, the dynamic condition and the boundary condition that $U = 0$ [from (4)] are applied; at the north and south noncorner

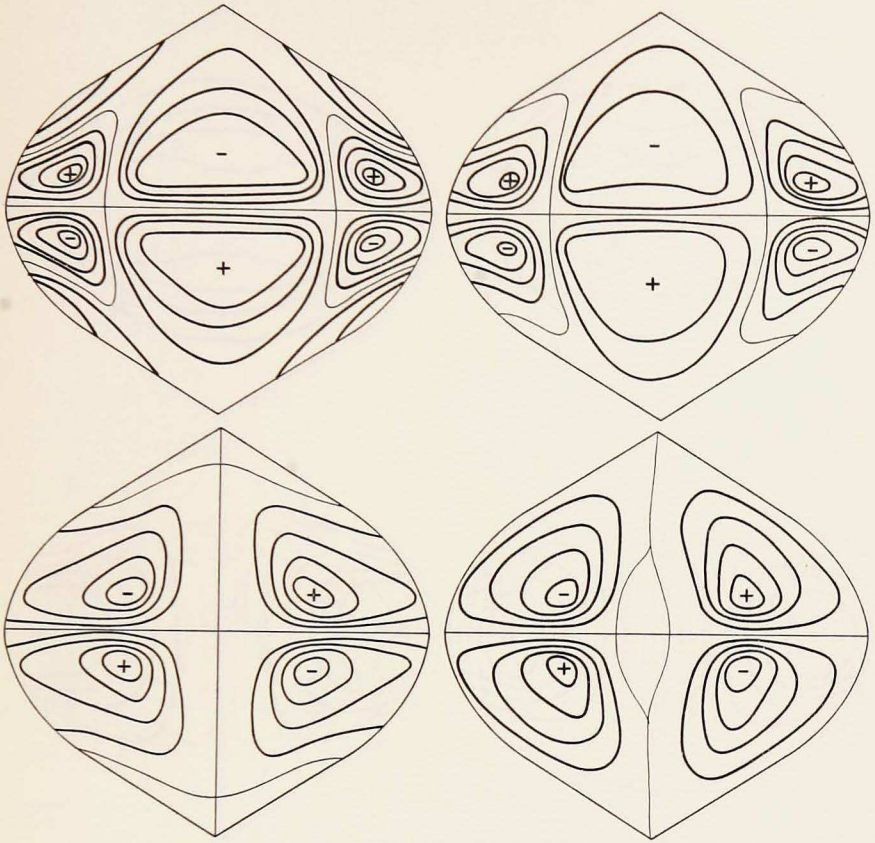

Figure 3a (left). Planetary oscillation $(1,1,p)$ with period = 52.2 hr for a hemisphere with $h = 4$ km everywhere. Figure 3b (right). Planetary oscillation $(1,1,p)$ with period = 51.6 hr for a hemisphere with a coastal shelf. Above: Re(Z). Below: Im(Z).

boundary points, the dynamic condition and the condition that $V = 0$ [from (5)] are applied; and, at corner points, $U = 0$, $V = 0$, and the dynamic condition are used.

Each condition is put in finite-difference form. This is done by replacing derivatives in (4), (5), (6) with three-point central differences (as in Salvadori and Baron 1961; 80). It then becomes a linear homogeneous equation and only approximates the original condition. Central differences applied at the boundary and corner points involve points outside the boundaries. Dependence on these points is eliminated algebraically, so that there are as many equations as there are unknown values of the dependent variable and as there are grid points. The equations are homogeneous and the coefficients of the dependent variable are polynomials in the frequency parameter, λ.

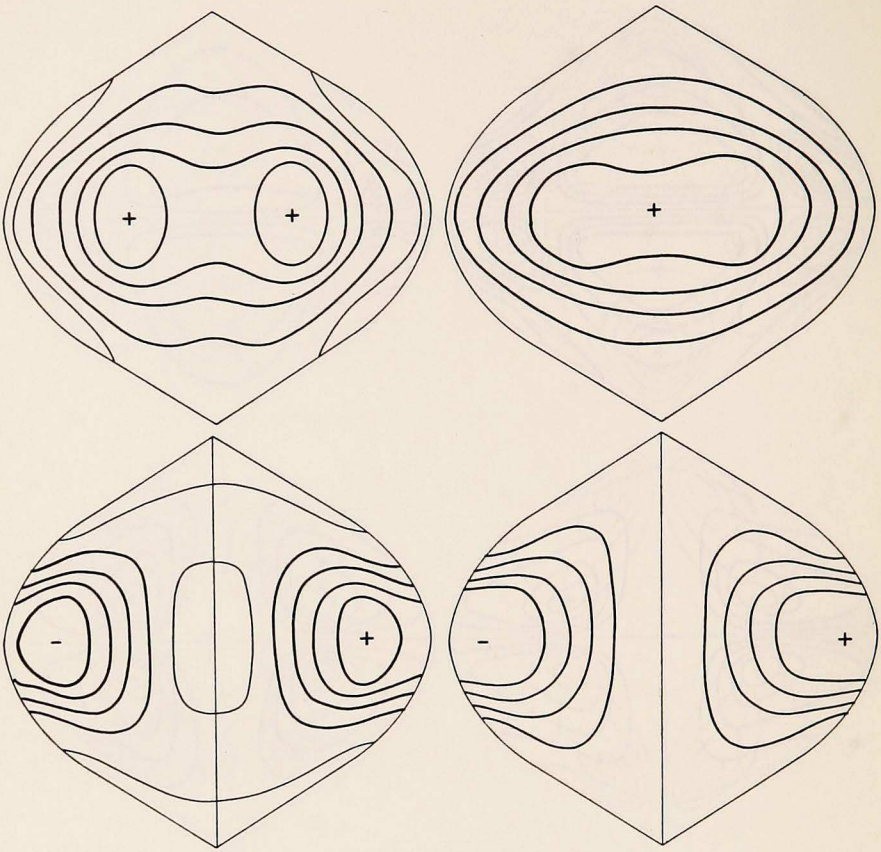

Figure 4a (left). Gravity oscillation (1,1,g) with period = 44.3 hr for a hemisphere with h = 4 km everywhere. Figure 4b (right). Gravity oscillation (1,1,g) with period = 43.9 hr for a hemisphere with a coastal shelf. Above: Re(Z). Below: Im(Z).

This is now a general eigenvalue problem, and nontrivial solutions of the matrix equation,

$$A(\lambda)\,\mathrm{Z} = 0, \tag{7}$$

are sought. A is the matrix of coefficients and Z is a vector whose elements are values of the sea-surface oscillation at each grid point. For a grid of n points, A is an n-by-n matrix and Z is an n-by-1. A, Z, and λ may be complex.

A nearly hemispherical basin, centered on the equator, is used to study the effects on long waves of a shelf at the boundaries. At first, solutions are found for a basin that is 4 km deep everywhere. They can be tentatively identified from studies (Longuet-Higgins and Pond 1970, Mofjeld and Rattray 1971, Christensen 1972). Then, each solution is followed as a shelf is added at the

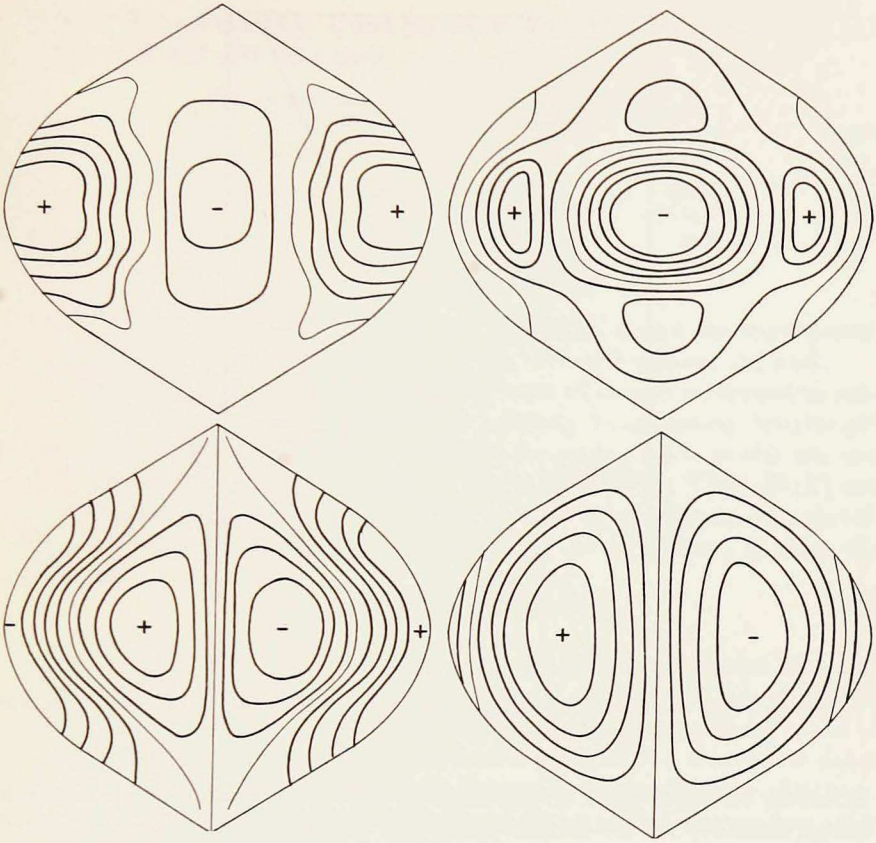

Figure 5a (left). Gravity oscillation (2,2,g) with period = 21.7 hr for a hemisphere with $h = 4$ km everywhere. Figure 5b (right). Gravity oscillation (2,2,g) with period = 25.6 hr for a hemisphere with a coastal shelf. Above: Re(Z). Below: Im(Z).

boundaries. Changes in frequency and in wave form are attributed to the addition of the shelf.

A rectangular 8-by-8 grid of points represents the basin. The northern and southern rows of points are at 89°N and 89°S, respectively, so that the points are separated by 178/7 degrees in the θ direction. Western and eastern boundaries are meridians, 180 degrees apart, so that points are separated by 180/7 degrees in the φ direction.

The shelved basin has a final bottom configuration of the form

$$H' = 4.0(1 - Re^{-Y^2/2})(1 - Re^{-X^2/2})\,\text{km}, \tag{8}$$

where H' is the final depth configuration, R determines the depth at the boundaries, and X and Y are scale distances from the boundaries. For an 8-by-8 grid,

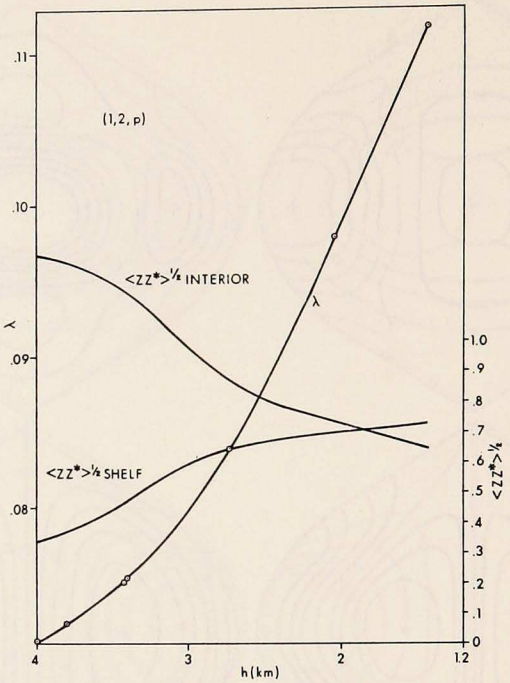

Figure 6. Values of λ and wave amplitude on and off the shelf as a function of the minimum shelf depth for the $(1,2,p)$ oscillation.

R and the scale of X and Y are chosen so that the final configuration has a depth of approximately 1.2 km on the boundary at the equator. The shelf is confined to the boundary points and to the line of points adjacent to the boundary points. The final configuration is contoured in Fig. 1. A shelf of this form is shallower at the corners than elsewhere on the boundary.

Modes of Oscillation. Four solutions were followed as the shelf was added. They are tentatively identified and ordered according to frequency as follows:

$(1,2,p)$ the first symmetric planetary mode;
$(1,1,p)$ the first antisymmetric planetary mode;
$(1,1,g)$ the first symmetric gravity (Kelvin) mode;
$(2,2,g)$ the second symmetric gravity (Kelvin) mode.

The two numerical indices refer to indices of spherical harmonics, as described by Christensen (1973), and are in agreement with Longuet-Higgins and Pond (1970). Symbol p or g refers to a planetary or gravity wave, respectively, and the symmetry refers to the configuration of Z about the equator.

Table I. Wave frequency, λ, and period, T, for the modes of oscillation in a basin with and without a shelf.

Mode	Flat-bottom case λ	Flat-bottom case T (hrs)	Shelved-bottom case λ	Shelved-bottom case T (hrs)	Figure no.
$(1,2,p)$	.071184	168.6	.11175	107.4	2
$(1,1,p)$	.22976	52.2	.23239	51.6	3
$1,1,g)$	.27095	44.3	.27335	43.9	4
$(2,2,g)$	.55315	21.7	.46845	25.6	5

Table I lists the nondimensional-wave frequency, λ, and the wave period, T, in hours for the four modes in the basin, with and without the shelf.

In Figs. 2 through 5, surface topographies are contoured on sinusoidal projections of a hemisphere. Two plots are necessary to adequately describe the surface wave. It is convenient to represent the surface wave as the real and imaginary parts of a complex quantity: $Re(Z)$ and $Im(Z)$. Then $Re(Z)$ and $Im(Z)$ are the wave at two phases, different in time by a quarter of a period. The sea-surface topography can be constructed for any phase, ν, using the relationship

$$Z(\nu) = \cos \nu \; Re(Z) + \sin \nu \; Im(Z) . \tag{9}$$

The difference in frequencies and surface topographies between the solutions for the flat-bottom case and the solutions in Christensen (1973) may be attributed to the differences in computational techniques, to the coarseness of the 8-by-8 grid, and to slight differences in boundary shapes. Because no direct correspondence between the two sets of solutions has been made, the identification of modes is tentative, only a comparison of frequencies and sea-surface topographies having been made.

For the planetary modes, frequencies increase as a shelf is added; for the gravity modes, they apparently can either increase or decrease. The shape of the surface wave changes very little for the $(1,1,p)$ mode (cf. Figs. 3a and 3b) and for the $(1,1,g)$ mode (cf. Figs. 4a and 4b). For the $(1,2,p)$ mode, the amplitude of the surface wave appears to increase near the boundaries and decreases in the interior (cf. Figs. 2a and 2b). The $(2,2,g)$ mode gives an opposite response. Initially the wave amplitude is high on the boundary at the equator but moves to the interior with the addition of the shelf (cf. Figs. 5a and 5b).

The migration of the waves on and off the shelf is seen more clearly by computing the rms amplitude of the wave on the shelf and in the interior. The shelf alters the depth at the boundary points and at the points adjacent to the boundary points. For an 8-by-8 grid, this involves 28 points. The other 36 points are at points with a depth of 4 km. Curves of

$$\langle ZZ^* \rangle^{1/2}_{\text{SHELF}} \quad \text{and} \quad \langle ZZ^* \rangle^{1/2}_{\text{INTERIOR}},$$

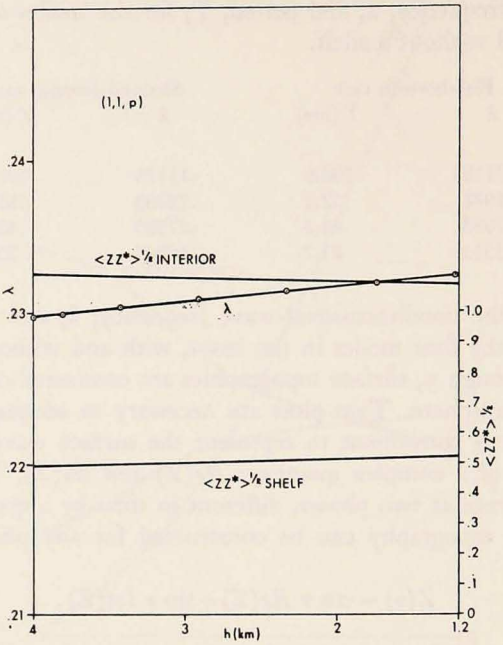

Figure 7. Values of λ and wave amplitude on and off the shelf as a function of the minimum shelf depth for the $(1,1,p)$ oscillation.

as well as of λ, are plotted against the depth on the boundary at the equator for the $(1,2,p)$ mode (Fig. 6), the $(1,1,p)$ mode (Fig. 7), the $(1,1,g)$ mode (Fig. 8), and the $(2,2,g)$ mode (Fig. 9). Z^* is the complex conjugate of Z; the brackets indicate mean quantities weighted according to the surface area.

The results of these computations verify the observed behavior of the surface waves. The $(1,1,p)$ and $(1,1,g)$ modes show little migration of wave amplitude, and their frequencies change only slightly as the shelf is added. In the case of the $(1,2,p)$ mode, the wave amplitude increases on the shelf and decreases in the interior; the frequency increases sharply. For the $(2,2,g)$ mode, exactly the opposite response is seen: the wave amplitude decreases on the shelf and increases in the interior, and the frequency decreases as the shelf is added. The two planetary modes respond in a similar way, and so do the two gravity modes.

For the $(1,2,p)$ and $(2,2,g)$ modes, Figs. 6 and 9 show the wave migrations to be more responsive to shelf changes for boundary depths between 2 and 3.5 km. Frequency changes are less for boundary depths that are greater than 3.5 km; they are greater and appear to be linear functions of boundary depths for values of less than 3.5 km. Apparently the wave migrations are nearly complete at the final boundary depth of 1.2 km whereas the frequencies would continue to change linearly if the shelf were made more shallow.

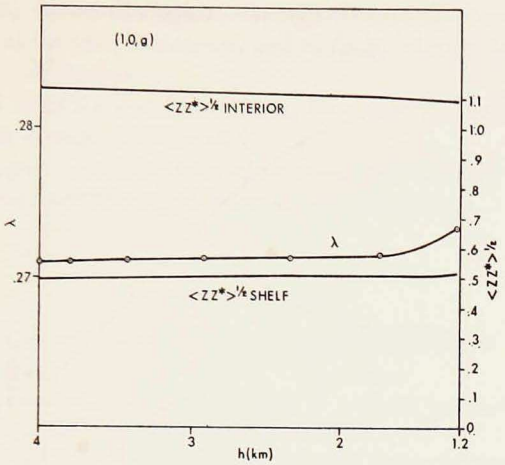

Figure 8. Values of λ and wave amplitude on and off the shelf as a function of the minimum shelf depth for the $(1,1,g)$ oscillation.

The behavior of the planetary modes may relate to theories of Buchwald (1969) and Longuet-Higgins (1968). They have found that long waves propagating along discontinuities in depth, with the wave amplitude dropping off exponentially to either side, are possible.

Conclusions. Normal modes can respond in several ways to the addition of a shelf at the boundaries of an otherwise constant-depth hemispherical basin. The mean depth is less with a shelf, and according to curves of λ versus $H^{1/2}$ of Longuet-Higgins and Pond (1970), a decrease in depth always results in a decrease in λ. Therefore, one response to the shelf might be a decrease in frequencies.

Bottom features can act as a wave guide to long waves (Longuet-Higgins 1968, Buchwald 1969). For planetary modes particularly, the addition of a shelf would result in an increase in the wavelength of the modes. In going from the eastern boundary to the western boundary, waves moving along the shelf would travel a longer distance than if they moved through the central basin. In the case of planetary waves, an increase in wavelength means an increase in λ. But in gravity waves, an increase in wavelength results in a decrease in λ. This offers a second way for modes to respond to the addition of the shelf.[2]

2. One of the referees prefers to summarize the effects of variable bathymetry by categorizing the effects into four types:

(i) The enhanced beta effect, since the potential planetary vorticity, f/h, varies because of both the Coriolis parameter, f, and the depth, h;

(ii) The smaller phase speed $c = (gh)^{1/2}$ of gravity waves near the boundaries, affecting particularly the gravity modes;

(iii) The smaller decay rate, f/c, for Kelvin modes near the boundaries, affecting also Poincaré modes;

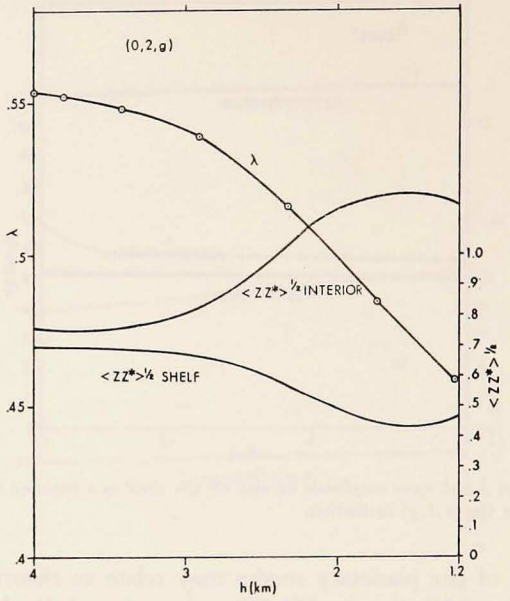

Figure 9. Values of λ and wave amplitude on and off the shelf as a function of the minimum shelf depth for the $(2,2,g)$ oscillation.

Of the four numerical solutions deformed, two respond strongly to a shelf: the $(1,2,p)$ mode and the $(2,2,g)$ mode. It is of interest to speculate about the probable causes of these responses. In the case of the $(2,2,g)$ mode, the wave moves away from the boundaries with the addition of the shelf (Fig. 9). This would effectively decrease the wavelength and increase λ. But λ decreases in accordance with a decrease in depth. This is not surprising, for Kelvin-type gravity waves are closely associated with the boundaries. In adding a shelf, depth is decreased near the boundaries.

On the other hand, the $(1,2,p)$ wave moves onto the shelf (Fig. 6). Without the shelf, this mode had highs and lows moving through the central basin with essentially no motion near the boundaries. Therefore, this represents a fundamental alteration in the behavior of the mode. In accordance with an increase in wavelength, the frequency increases with the addition of the shelf.

Acknowledgments. I thank Gordon W. Groves for his invaluable support, advice, and contributions throughout the study. I am also grateful to M. S.

(iv) The effects on the length scale $(c/\beta)^{1/2}$, which determines whether the oscillations are equatorially trapped.

Examples of each effect of variable bathymetry can be seen in the figures. For example, the equatorial trapping can be seen in Fig. 3 for $(1,1,p)$. The mode $(1,2,p)$ in Fig. 2a is not equatorially trapped in the constant depth ocean, and the corresponding mode with bathymetry seems to propagate along the boundary rather than along the equator.

Longuet-Higgins, Brent Gallagher, George Platzman, George Carrier, and Merl Hendershott for their assistance, and to Gary Meyers for checking some of the most difficult algebra.

I thank Ethel McAfee and Rita Pujalet for editorial help; the figures were prepared by Dick Rhodes and his staff.

Most of the support for this work came from the National Science Foundation through grants GA-1117, GP-4254, and GA-17137.

REFERENCES

Buchwald, V. T.
1969. Long waves on ocean ridges. Proc. roy. Soc. London, (*A*)*308*: 343–354.

Christensen, Jr., Niels
1972. Numerical simulation of free oscillations of enclosed basins on a rotating earth. Hawaii Inst. Geophys., Univ. of Hawaii. Rep. 72–9; 181 pp.

1973. On free modes of oscillation of a hemispherical basin centered on the equator. J. mar. Res., *31*(3): 168–174.

Eckart, Carl
1960. Hydrodynamics of oceans and atmospheres. Pergamon Press, New York. 290 pp.

Hough, S. S.
1898. On the application of harmonic analysis to the dynamical theory of the tides. II: on the general integration of Laplace's tidal equations. Phil. Trans., (*A*)*191*: 139–185.

Lamb, Horace
1945. Hydrodynamics. Dover Publications, New York, 738 pp.

Longuet-Higgins, M. S.
1968. On the trapping of waves along a discontinuity of depth in a rotating ocean. J. fluid Mech., *31*(3): 417–434.

Longuet-Higgins, M. S., and G. S. Pond
1970. The free oscillations of fluid on a hemisphere bounded by meridians of longitude. Phil. Trans., (*A*)*266*: 193–223.

Mofjeld, H. O., and Maurice Rattray, Jr.
1971. Free oscillations in a beta-plane ocean. J. mar. Res., *29*(3): 281–305.

Rhines, P. B.
1969. Slow oscillations in an ocean of varying depth. Part 1. Abrupt topography. J. fluid Mech., *37*: 161–190.

Salvadori, M. G., and M. L. Baron
1961. Numerical methods in Engineering. Prentice-Hall, Inc., Englewood Cliffs, N.J. 302 pp.

Veronis, George
1966. Rossby waves with bottom topography. J. mar. Res., *24*: 338–349.